ATLANTIS PRESS

Advances in Engineering Research, volume 120

International Forum on Energy, Environment Science and Materials (IFEESM 2017)

Effects of surface treatment on the electrocatalytic performance of Spinel $NiCo_2O_4$ and Carbon Nanotubes composite catalysts

Yangbo Chen[1], Yuwei Tang[1], Zhoumiao Liao[1], Xiaoyang Chen[1], Juan Wang[1*]

[1]School of Chemical Engineering, Nanjing University of Science and Technology, Nanjing 210094 (PR China).

Email: wangjuan304@njust.edu.cn

Keywords: Surface treatment; Spinel $NiCo_2O_4$; Carbon Nanotubes; Oxygen reduction reaction; Oxygen evolution reaction; Electrocatalyst.

Abstract: How to develop high-efficient and low-cost electrocatalysts for the oxygen reduction reaction (ORR) and oxygen evolution reaction (OER) is urgent in fuel cell and metal-air batteries. What we are going to introduce is how to improve the performance of catalyst for ORR and OER under different acid treatment conditions. Spinel $NiCo_2O_4$ and carbon nanotubes (NC-0) composites have been synthesized via a facile hydrothermal method without using high temperature and the result samples were treated using nitric acid for 1h, 2h and 3h， which are named NC-*x* (*x*=1,2 and 3) respectively. Comparing the untreated composite (NC-0) with NC-3, the ORR current density is increased from 2.1 mA / cm^2 to 4.2 mA / cm^2 and OER current density is reduced from 13.3 mA / cm^2 to 8.0 mA / cm^2. The result would enlighten and promote directional synthesis of different performance electrochemical catalyst.

Introduction

Rapid economic growth and social development is leading to a large gap between the reduced availability of fossil fuels and increased energy demands. With the continuous depletion of fossil fuels and concerns about climate change such as global warming, it's a pressing need to develop renewable and sustainable energy sources. Therefore, the research of electrogenic reactors such as metal-air cells and microbial fuel cells is speeding up nowadays [1-3].

Much effort has been invested to enhance energy production in the electrogenic reactors, but how to make the improvement in the cathode catalysts has still remained as one of the largest challenges in their application. Especially, bifunctional catalysts play an important role in those reactors for oxygen reduction reaction (ORR) and oxygen evolution reaction (OER) [4-6].

Platinum and its alloys are used as catalyst for ORR [7-9], while ruthenium and iridium-group metals are for OER but show poor performance for ORR [10, 11]. At the same time, these noble metals have problems of scarcity, high cost and limited stability. By contrast, several non-noble transition metals such as Mn, Co and Ni and their oxides are reported to be efficient and low-cost catalysts [12, 13]. Former members of our group have done some research and achieved some results. For example, Hu et al have reported that carbon-supported spinel nanoparticle $MnCo_2O_4$ showed remarkable ORR catalytic activity, which was prepared by a two-step solvothermal method [14]. And nickel-cobalt spinel ($NiCo_2O_4$) is another important member of the valence oxide with spinel structure, which was also reported to have relatively high electrical conductivity and stability [15]. Nanostructured $NiCo_2O_4$ exhibits better electronic conductivity and higher electrochemical activity than NiO and Co_3O_4 [16, 17]. The presence of two solid couples (Ni^{3+}/Ni^{2+} and Co^{3+}/Co^{2+}) in the spinel structure enables $NiCo_2O_4$ to show a great electrocatalytic activity [18].

Various types of configuration enable nickel-cobalt spinels to have different performance from each other. This means that the structure plays a crucial part on their capacitive performance. As far as we know, nickel-cobalt spinels with the following configurations have been synthesized: nanosheet [19, 20], nanoplate [21-23], nanoflower [24, 25], nanotube [26-28], nanowire [29, 30], and urchin-like nanostructures [31, 32]. In addition, it was found that synthesis method and process condition of spinel oxides can significantly affect their electrochemical characteristics [33]. To further enhance oxygen electrocatalytic activity, Xu's group has studied the theory of how the

transition-metal cations functions in spinel oxides through changing the calcination temperature during the synthesis process [34].

Furthermore, it has been reported that the composites of metal oxides and carbon materials have high electrocatalytic performance [35, 36]. Multiwalled carbon nanotubes (CNTs) have attracted much more preference for their superior electrical conductivity and structural flexibility and are proved to be promising substrates for supporting nanocrystal catalysts.

With the experimental experience and the inspiration from Xu's group, we aim to explore the effects of different surface treatment conditions on the electrochemical properties of spinel-CNTs composite catalysts for ORR/OER. The prepared spinel-CNTs composites with surface treatment conditions have been examined in terms of electrochemical reactions.

Results and discussion

One untreated $NiCo_2O_4$-CNTs catalyst (NC-0) and three $NiCo_2O_4$-CNTs catalysts which were treated with 1 M nitric acid for 1h (NC-1), 2h (NC-2) and 3h (NC-3) respectively were identified by XRD and their patterns were shown in Figure 1. In all the images, the standard diffraction peak of $NiCo_2O_4$ (PDF # 20-0781) is presented. The Figure 1 (a) shows that the peaks of NC-0 are chaotic, and there are many other random peaks other than $NiCo_2O_4$ spinel peak whose signal is weak. But the diffraction peak of the carbon nanotube is not obvious, indicating that carbon nanotubes of NC-0 were covered with spinel instead of being exposed to the surface of the material. After nitric acid treatment, CNT are showed on the surface of the catalysts as shown in Figure 1 (b) (c) (d).

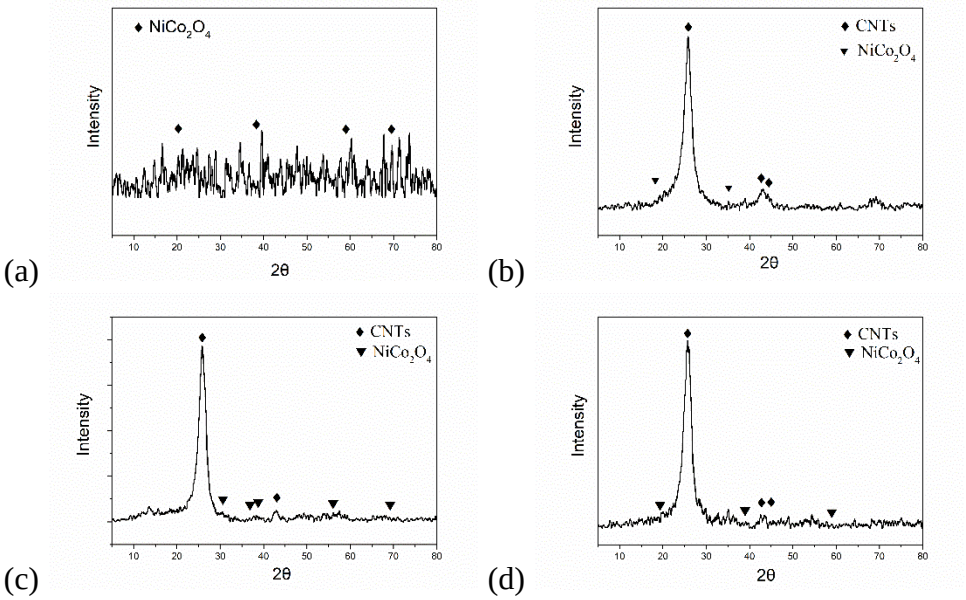

Figure 1. XRD patterns of NC-0(a), NC-1(b), NC-2(c), NC-3(d)

Figure 2 shows the TEM images of NC-0 and NC-3. As shown in the Figure 2 (a), the untreated sample (NC-0) is covered with a large number of spinel oxides which appear in random order on its surface. The outline of carbon nanotubes can be observed as well. It also shows that different sizes of spinel oxide particles attached to the surface of the carbon nanotubes from Figure 2 (b). As shown in Figure 2 (c) and (d), surface of the carbon nanotubes is smooth and there is nothing attached to it anymore. However, there are some black particles at the inwall of the carbon nanotubes and the diameter of most particles is equivalent to that of the pipe wall. It is supposed that some defects appeared on the surfaces of carbon nanotubes under the effect of strong oxidizer. In the later process, these defects gave a chance to a small number of smaller particles to stick in.

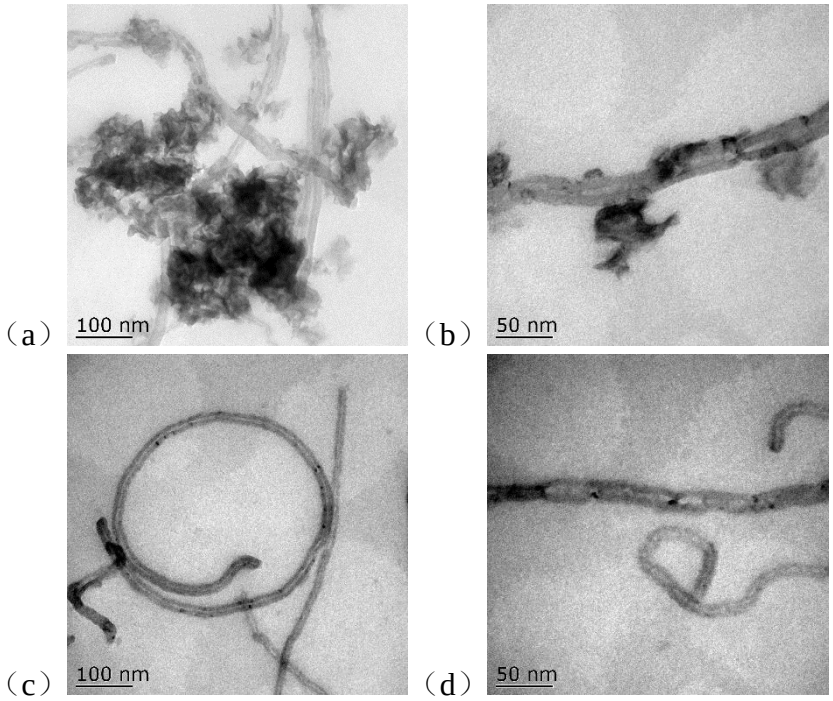

Figure 2. (a) & (b) TEM images of NC-0, (c) & (d) TEM images of NC-3

Different samples prepared under different conditions of before and after nitric acid treatment (NC-0 and NC-3) were analyzed by XPS photoelectron spectroscopy. Figure 3 (a) (b) (c) show the full spectrum of NC-0, Ni(2p) and Co (2p) XPS spectra while Figure 3 (d) (e) (f) show the full spectrum of NC-3, Ni(2p) and Co (2p) XPS spectra.

Figure 3 (a) shows that sample NC-0 contains Ni, Co, O, C and N elements: Ni, Co, O were from spinel and C was from carbon nanotube and N is probably from nitrogen-containing functional groups such as nitro because of nitric acid in the synthesis process. This complicated spectrum indicates that the sample contains more than one forms of catalyst. Figure 3 (b) and (c) are the XPS spectra of Ni (2p) and Co (2p) of sample NC-0 respectively. Two distinct main peaks and satellite peaks can be seen from Figure 3 (b), with 855.7eV and 857.0eV corresponding to Ni^{2+} and 873.1eV corresponding to Ni^{3+}. Similarly, there are also two obvious main peaks and satellite peaks, with 780.9 eV, 796.8eV and 798.2eV corresponding to Co^{2+} and 782.3eV corresponding to Co^{3+} in the Figure 3 (c). It can be seen after nitric acid treating, the signals of Ni and Co are weakened but the signal of C is strengthened, indicating that part of the $NiCo_2O_4$ spinel oxides on the surface of the carbon nanotubes was cleaned out, originally was enshrouded carbon nanotubes from Figure 3 (d). There are obvious main and satellite peaks of Ni 2p in Figure 3 (e), of which 855.5 eV and 872.5 eV corresponding to Ni^{2+} and 856.3 eV and 872.5 eV corresponding to Ni^{3+} [22]. Similarly, in Figure 3 (f), 780.7 eV & 795.0 eV and 781.0 eV & 796.5 eV respectively correspond to Co^{2+} and Co^{3+} [37]. To conclude, the existence of different elements of Ni and Co makes the catalyst have great electrochemical properties. Moreover, we find that Ni/Co ratio of sample NC-0 is close to 1:2, which is the theory spinel ratio. Ni/Co ratio of sample NC-3 is close to 1:1 but Ni/O or Co/O ratio is reaching up to 1:26. It is assumed that after nitric acid treatment, a large amount of spinel on the surface was dissolved in acid, while only a small number of Ni or Co oxides remained on the surface or the interior of the carbon nanotubes without being washed away. At the same time, the oxygen-containing functional groups on the surface of acidified carbon nanotubes have increased the proportion of O atom.

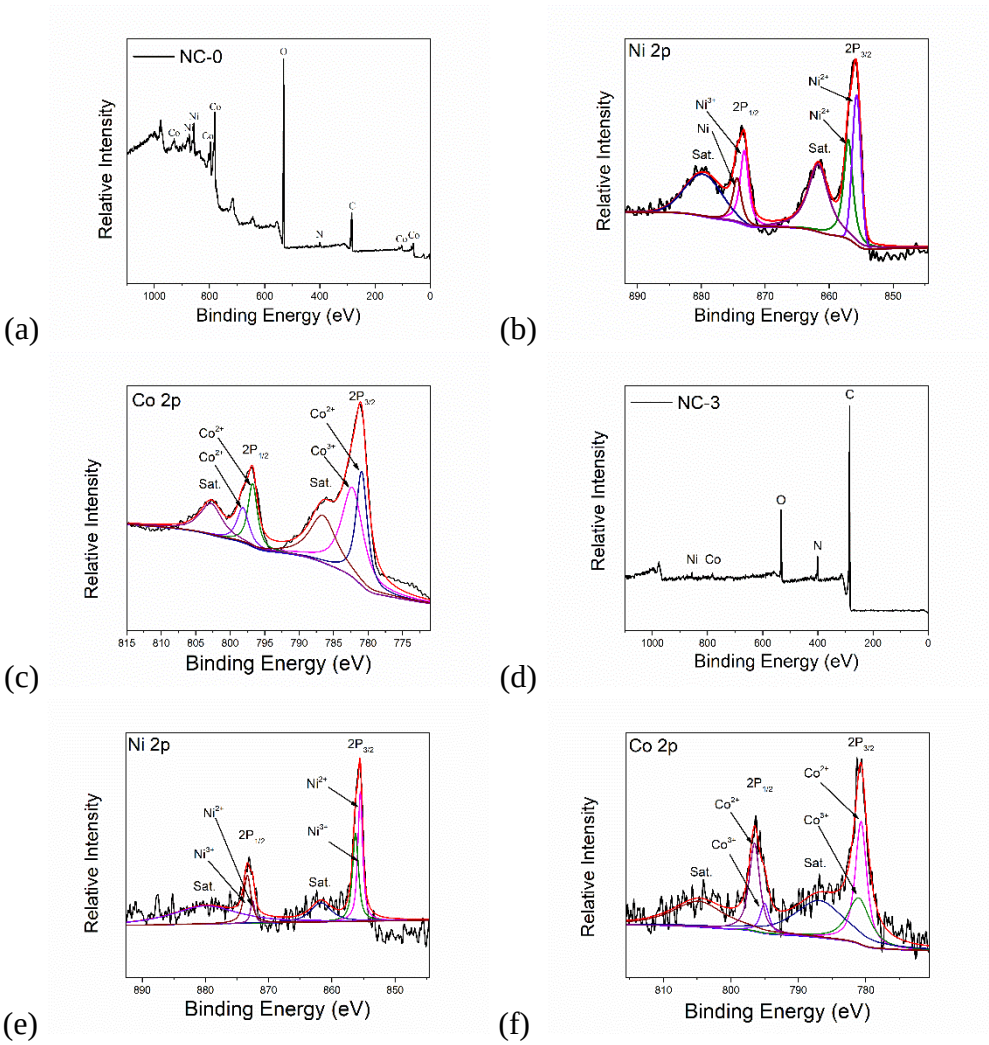

Figure 3 XPS spectra of (a)(c) Ni 2p, (b)(d) Co 2p for NC-0 and NC-3

We further studied the nitric acid treatment conditions and the influence of the surface spinel of CNTs on electrochemical properties. Mixed isopropyl alcohol, H_2O, Nafion into a solution with the ratio of 200: 800: 40.Took 1 ml of the above solution and then mixed up with 10 mg sample, and then we could get a homogeneous suspension after the mixture was sonicated for about 30 minutes. Measured 10μL suspension by pipette gun and then dropped it on the surface of the polished glass electrode after drying. Finally, we got the testing electrode after drying overnight. The electrochemical test was proceeded in the CHI660D electrochemical workstation with three-electrode system. The working electrode was a glassy carbon electrode(Φ=5mm), the reference electrode was Ag / AgCl, the contrast electrode is a Pt electrode and the electrolyte solution is 0.1mol / L KOH solution.

The preparation of the obtained spinel carbon nanotube composite catalyst using 1M nitric acid was performed without the simultaneous long nitric acid treatment, and the ORR and OER activity was detected, as shown in the Figure (a) (b). As can be seen from the figure, the initial potential and current density decreased after nitric acid treatment in the OER test, while in ORR test, the nitric acid treatment has resulted in potential decrease and the current density increased. We made the following hypothesis: under the condition of higher spinel content, for OER is relatively good, but after washing, the spinel content decreased, makes the exposed surface coated carbon nanotubes, due to its superior conductivity, combined with excellent electrochemical performance of spinel, ORR performance was improved. When we observe ORR and OER curves under different washing conditions, we find that they are not very different. This may be that the acid in the concentration of the acid can quickly wash away the spinel of the catalyst surface, so that the samples we get tend to be consistent.

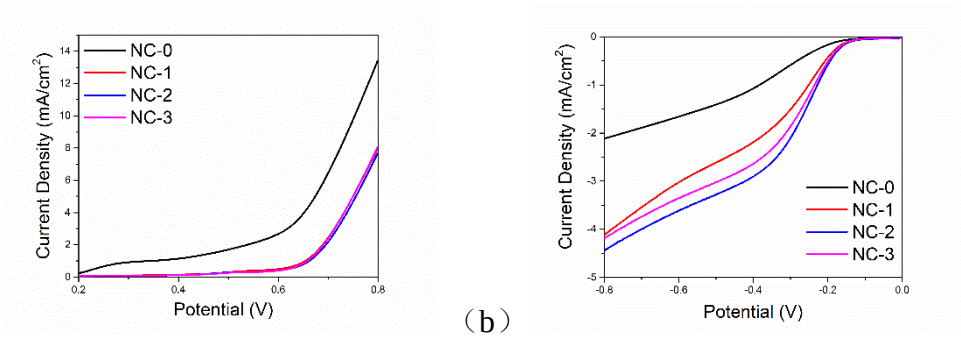

Figure 4 RED polarization plots of different samples in different washing conditions

We tested the rotation disc polarization curves of different samples at different speeds, as shown in Figure (a) (b) (c) (d). It can be observed that with the increase of rotational speed, the corresponding current density also increased, indicating that the rotating speed is helpful to reduce the diffusion.

To explore the mechanism of this process, we calculated the number of transferred electron through the Koutecky-Levich equation. The calculation process is as follows:

$$J^{-1}=J_L^{-1}+J_K^{-1}=（B\,\omega^{1/2}）^{-1}+J_K^{-1} \quad （1）$$

$$B=0.2nFC_0(D_0)^{2/3}\,\upsilon^{-1/6} \quad （2）$$

$$J_K=nFkC_0 \quad （3）$$

Among them, J represents measured electric current density; J_L represents diffusion limited electric current density; J_K represents power limited electric current density; n is the number of transferred electron; F is Faraday constant (96485 C/mol); D_0 is diffusion coefficient (1.9×10^{-5} cm^2s^{-1}); ω is electrode speed; υ is electrolyte dynamic viscosity (0.01 cm^2s^{-1}); C0 is the oxygen concentration in solution (1.2×10^{-3}M); k is the electron transfer constant. The K-L curve is made according to the formula (6) (7) (8) and the measured LSV curve data as shown in Figure. After calculation, the number of transferred electron for four catalysts was 3.75, 3.63, 3.35 and 2.99 respectively.

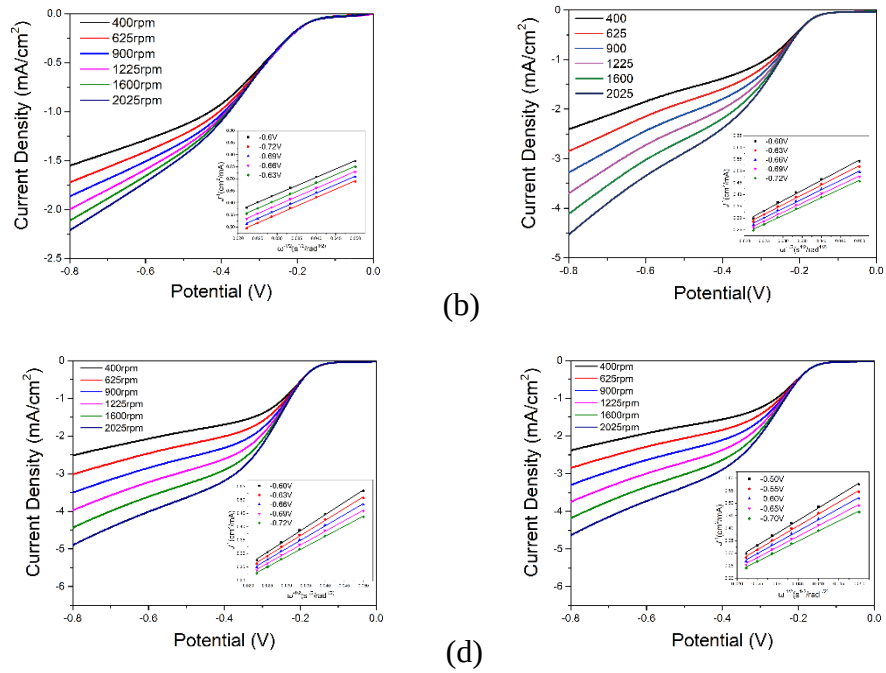

Figure5 LSV for samples in different rotation speeds

Experimental

Pre-processing of CNTs

CNTs were provided by Xian Feng Nano Co., Ltd. 500mg of CNTs was dispersed in 50ml of 68% HNO_3, refluxing at 140℃ for 12h. After that, CNTs was separated by centrifugal and washed three

times with DI water and then once with ethanol. It is dried in a vacuum oven at 80℃ overnight. The processed CNTs was named p-CNTs.

Preparation of NC-x

The catalyst was prepared using the starting precursor of $NiSO_4 \cdot 6H_2O$, $NiSO_4 \cdot 6H_2O$,ascorbic acid, ammonia solution and p-CNT. In a typical synthesis, the stoichiometric amount of $NiSO_4 \cdot 6H_2O$ (2mmol), $NiSO_4 \cdot 6H_2O$ (4mmol) and ascorbic acid (4mmol) were dissolved in 30 mL of water. Further, 50 mg of p-CNT was added into the former mixed solution. 2.4ml ammonia was added to adjust pH. After that, the solution was transferred into Teflon lined stainless steel container and kept at 120℃ for 12h under hydrothermal treatment. The obtained powder was washed by DI water for three times and ethanol for one time and dried in vacuum at 80℃ for 12h. Named it with NC-0. Treat NC-0 with nitric acid for 1, 2, 3 hours separately and wash them by DI water and ethanol.After being dried in vacuum at 80℃ for 12h we can get three samples named with NC-1, NC-2, NC-3.

Conclusions

Through a traditional hydrothermal method, Ni-Co spinel oxides and other tiny particles successfully attached to the carbon nanotubes. Particles of NC-0's surface exist a variety of structures, such as $NiCo_2O_4$, Co_3O_4, Ni. By a sample nitric acid treatment, we found that the catalyst surface has experienced drastic changes; almost all of the oxide was released from the surface of the carbon nanotubes. The remaining carbon nanotubes' wall is attached with nickel. The reason why nickel is attached to carbon nanotubes is because pre-treatment of carbon nanotubes. We characterized the ORR and OER properties of the catalysts with linear sweep voltammetry (LSV). Comparing NC-0 and NC-3, the ORR current density has doubled and the OER current density is reduced from 13.3 mA/cm^2 to 8.0 mA/cm^2. Similarly, we compared samples for different nitric acid treatment times and we found no significant difference in ORR and OER performance. Through this study, we can directionally prepare transition metals / carbon nanotubes composite catalysts with different electrochemical properties

ACKNOWLEDGMENTS

This work was financially supported by the Undergraduate Research Training "Millions Talents" Plan , the Extra-curricular Academic Scientific Research Fund of Nanjing University of Science and Technology.

Reference

1. Kodali, M.; Santoro, C.; Herrera, S.; Serov, A.; Atanassov, P., Journal of Power Sources 2017, 366, 18-26.
2. Zhu, N.; Lu, Y.; Liu, B.; Zhang, T.; Huang, J.; Shi, C.; Wu, P.; Dang, Z.; Wang, R., Journal of Nanoparticle Research 2017, 19 (10).
3. Zhao, Z.; Li, M.; Zhang, L.; Dai, L.; Xia, Z., Advanced Materials 2015, 27 (43), 6834-+.
4. Zhang, J.; Zhao, Z.; Xia, Z.; Dai, L., Nature Nanotechnology 2015, 10 (5), 444-452.
5. Qian, Y.; Hu, Z.; Ge, X.; Yang, S.; Peng, Y.; Kang, Z.; Liu, Z.; Lee, J. Y.; Zhao, D., Carbon 2017, 111, 641-650.
6. Zhao, A.; Masa, J.; Xia, W.; Maljusch, A.; Willinger, M.-G.; Clavel, G.; Xie, K.; Schloegl, R.; Schuhmann, W.; Muhlert, M., Journal of the American Chemical Society 2014, 136 (21), 7551-7554.
7. Nigam, S.; Majumder, C., Physical Chemistry Chemical Physics 2017, 19 (29), 19308-19315.
8. Wu, J.; Gross, A.; Yang, H., Nano Letters 2011, 11 (2), 798-802.
9. Carpenter, M. K.; Moylan, T. E.; Kukreja, R. S.; Atwan, M. H.; Tessema, M. M., Journal of the American Chemical Society 2012, 134 (20), 8535-8542.
10. Grimaud, A.; Demortiere, A.; Saubanere, M.; Dachraoui, W.; Duchamp, M.; Doublet, M. L.; Tarascon, J. M., Nat. Energy 2017, 2 (1), 10.

11. Jung, H. G.; Jeong, Y. S.; Park, J. B.; Sun, Y. K.; Scrosati, B.; Lee, Y. J., Acs Nano 2013, 7 (4), 3532-3539.
12. Bosch-Jimenez, P.; Martinez-Crespiera, S.; Amantia, D.; Della Pirriera, M.; Forns, I.; Shechter, R.; Borras, E., Electrochimica Acta 2017, 228, 380-388.
13. Bo, X.; Zhang, Y.; Li, M.; Nsabimana, A.; Guo, L., Journal of Power Sources 2015, 288, 1-8.
14. Hu, D.; Wang, H.; Wang, J.; Zhong, Q., Energy Technology 2015, 3 (1), 48-54.
15. Zhang, G.; Lou, X. W., Scientific Reports 2013, 3.
16. Yang, J.; Yu, C.; Liang, S.; Li, S.; Huang, H.; Han, X.; Zhao, C.; Song, X.; Hao, C.; Ajayan, P. M.; Qiu, J., Chemistry of Materials 2016, 28 (16), 5855-5863.
17. Jadhav, H. S.; Kalubarme, R. S.; Roh, J. W.; Jung, K. N.; Shin, K. H.; Park, C. N.; Park, C. J., J. Electrochem. Soc. 2014, 161 (14), A2188-A2196.
18. Shengjie, P.; Yuxiang, H.; Linlin, L.; Xiaopeng, H.; Fangyi, C.; Srinivasan, M.; Qingyu, Y.; Ramakrishna, S.; Jun, C., Nano Energy 2015, 13, 718-26.
19. Mohamed, S. G.; Tsai, Y.-Q.; Chen, C.-J.; Tsai, Y.-T.; Hung, T.-F.; Chang, W.-S.; Liu, R.-S., Acs Applied Materials & Interfaces 2015, 7 (22), 12038-12046.
20. Peng, L.; Zhang, H.; Fang, L.; Bai, Y.; Wang, Y., Acs Applied Materials & Interfaces 2016, 8 (7), 4745-4753.
21. Wang, J.; Li, L.; Tian, H.; Zhang, Y.; Che, X.; Li, G., Acs Applied Materials & Interfaces 2017, 9 (8), 7100-7107.
22. Tong, X.; Chen, S.; Guo, C.; Xia, X.; Guo, X.-Y., Acs Applied Materials & Interfaces 2016, 8 (42), 28274-28282.
23. Peng, L.; Xiong, P.; Ma, L.; Yuan, Y.; Zhu, Y.; Chen, D.; Luo, X.; Lu, J.; Amine, K.; Yu, G., Nature Communications 2017, 8.
24. Chen, H.; Jiang, J.; Zhang, L.; Qi, T.; Xia, D.; Wan, H., Journal of Power Sources 2014, 248, 28-36.
25. Wang, L.; Al-Mamun, M.; Liu, P.; Wang, Y.; Yang, H. G.; Wang, H. F.; Zhao, H., Npg Asia Materials 2015, 7.
26. Yang, J.; Fujigaya, T.; Nakashima, N., Scientific Reports 2017, 7.
27. Xu, X.; Zhou, H.; Ding, S.; Li, J.; Li, B.; Yu, D., Journal of Power Sources 2014, 267, 641-647.
28. Li, L.; Cheah, Y.; Ko, Y.; Teh, P.; Wee, G.; Wong, C.; Peng, S.; Srinivasan, M., Journal of Materials Chemistry A 2013, 1 (36), 10935-10941.
29. Xu, K.; Li, S.; Yang, J.; Xu, H.; Hu, J., Journal of Alloys and Compounds 2016, 678, 120-125.
30. Li, Y.; Hasin, P.; Wu, Y., Advanced Materials 2010, 22 (17), 1926-+.
31. Liu, Z.-Q.; Xu, Q.-Z.; Wang, J.-Y.; Li, N.; Guo, S.-H.; Su, Y.-Z.; Wang, H.-J.; Zhang, J.-H.; Chen, S., International Journal of Hydrogen Energy 2013, 38 (16), 6657-6662.
32. Jin, C.; Lu, F.; Cao, X.; Yang, Z.; Yang, R., Journal of Materials Chemistry A 2013, 1 (39), 12170-12177.
33. Hamdani, M.; Singh, R. N.; Chartier, P., International Journal of Electrochemical Science 2010, 5 (4), 556-577.
34. Wei, C.; Feng, Z.; Scherer, G. G.; Barber, J.; Shao-Horn, Y.; Xu, Z. J., Advanced Materials 2017, 29 (23).
35. Peng, S.; Li, L.; Hu, Y.; Srinivasan, M.; Cheng, F.; Chen, J.; Acs Nano 2015, 9 (2), 1945-1954.
36. Shen, L.; Che, Q.; Li, H.; Zhang, X., Advanced Functional Materials 2014, 24 (18), 2630-2637.
37. Yang, S.; Wang, Z.; Cao, Z.; Mao, X.; Shi, M.; Li, Y.; Zhang, R.; Yin, Y., Journal of Alloys and Compounds 2017, 721, 482-491.